Phosphorus Metabolism-Related Genes Serve as Novel Biomarkers for Predicting Prognosis in Bladder Cancer: A Bioinformatics Analysis

#*Yang He [1,2], #*Abai Xu [2], *Li Xiao [3], *Ying Yang [4], *Boping Li [2], *Zhe Liu [2], *Peng Rao [2], *Yicheng Wang [2], ***Li Ruan [1], *Tao Zhang [1]*

1. *Department of Urology, Guangzhou Red Cross Hospital, Jinan University, Guangzhou, China*
2. *Department of Urology, Zhujiang Hospital, Southern Medical University, Guangzhou, China*
3. *Department of Medical Oncology, National Cancer Center/National Clinical Research Center for Cancer/Cancer Hospital & Shenzhen Hospital, Chinese Academy of Medical Sciences and Peking Union Medical College, Shenzhen, China*
4. *Department of Hematology, Guangzhou Red Cross Hospital, Jinan University, Guangzhou, China*

*Corresponding Authors: Emails: ruanli1978@126.com; zhtics@126.com
# These authors contributed equally to this work

Abstract

Background: Phosphorus metabolism might be associated with tumor initiation and progression. We aimed to screen out the phosphorus metabolism genes related to bladder cancer and construct a clinical prognosis model.

Methods: The dataset used for the analysis was obtained from TCGA database. GO and KEGG enrichment analyses were subsequently applied to differentially expressed genes. Consensus clustering was utilized, and different clusters of the tumor immune microenvironment and other features were compared. The phosphorus metabolism-related genes involved in prognosis were screened out by univariate Cox regression, LASSO regression and multivariate Cox regression analysis, and a nomogram was constructed. The performance of the nomogram was validated using TCGA dataset and the GEO dataset, respectively.

Results: Overall, 405 phosphorus metabolism-related differentially expressed genes from TCGA database were identified, which were associated with phosphorylation, cell proliferation, leukocyte activation, and signaling pathways. Two clusters were obtained by consistent clustering. After tumor immune microenvironment analysis, significant differences in immune cell infiltration between cluster 1 and cluster 2 were found. Four phosphorus metabolism-related genes (*LIME1, LRP8, SPDYA*, and *MST1R*) were associated with the prognosis of bladder cancer (BLCA) patients. We built a prognostic model and visualized the model as a nomogram. Calibration curves demonstrated the performance of this nomogram, in agreement with that shown by the ROC curves.

Conclusion: We successfully identified four phosphorus metabolism-related genes associated with prognosis, providing potential targets for biomarkers and therapeutics. A nomogram based on these genes was developed. Nevertheless, this study is based on bioinformatics, and experimental validation remains essential.

Keywords: Bladder cancer (BLCA); Phosphorus metabolism; Prognosis; Nomogram

Available at: http://ijph.tums.ac.ir

Introduction

The prevalence of BLCA (bladder cancer) is steadily increasing, positioning BLCA as the tenth most frequently diagnosed cancer globally. Furthermore, it stands as the second most prevalent malignant tumor within the urinary system, posing a significant threat to human health (1). Metastasis is one of the leading causes of death in patients with BLCA (2). The development, progression and metastasis of bladder cancer are the results of a complex set of biological mechanisms involving numerous genes and multiple signaling pathways. Therefore, screening for new biomarkers that are able to accurately predict prognosis and predict the sensitivity of treatment regimens can uncover their significance as biomarkers of tumorigenesis and progression as well as explore possible therapeutic targets. Enhancing the precision of patient risk identification is instrumental in differentiating individuals based on distinct risk stratifications, thereby mitigating the risk of unnecessary overtreatment.

Phosphorus is involved in the composition of cellular structures, genetic materials, enzymes, cell-signaling molecules and participates in the activation of molecules, energy production and storage, etc. Phosphorus is one of the most critical elements in living organisms and plays an essential role in the normal life activities of cells. However, phosphorus metabolism may also be linked to malignant tumors. Patients with different types of cancer consistently exhibit hyperphosphatemia (3). The GRH (growth rate hypothesis) proposes that the accelerated growth and proliferation of tumors require an increased presence of phosphorus-rich nucleic acids (4). A previous study showed that interstitial inorganic phosphate concentrations were higher in tumors than in normal tissues and in highly metastatic tumors than in non-metastatic ones, suggesting that disturbances in phosphorus metabolism may be a marker of tumor progression in the tumor microenvironment (4). Phosphate toxicity, resulting from disrupted phosphate metabolism, is linked to breast cancer and can trigger the development of tumors (5). It has been hypothesized that the metastatic migration of tumors may be phosphorus-driven (6). As depicted in previous research, increased phosphate levels in the tumor microenvironment stimulate cell signaling in tumor initiation and promote the development of new blood vessels in lung and breast cancer cells, which can result in tumor initiation and progression (5). Phosphates also participate in protein phosphorylation and serve as inducers of cell growth and proliferation through their role as mitogenic factors (7). In breast cancer, the presence of phosphate may stimulate the generation of hydrogen peroxide, thereby promoting the migration and adhesion of tumor cells (8). However, the relationship between phosphorus metabolism and tumor progression in BLCA remains unclear.

In this study, our objective was to explore the potential associations between phosphorus metabolism-related genes and the prognosis of bladder cancer patients, aiming to identify potential therapeutic targets. Additionally, we seek to investigate their influence on the TIME (tumor immune microenvironment) and construct a prognostic model for predicting survival of bladder patient, thereby guiding the selection of treatment strategies.

Materials and Methods
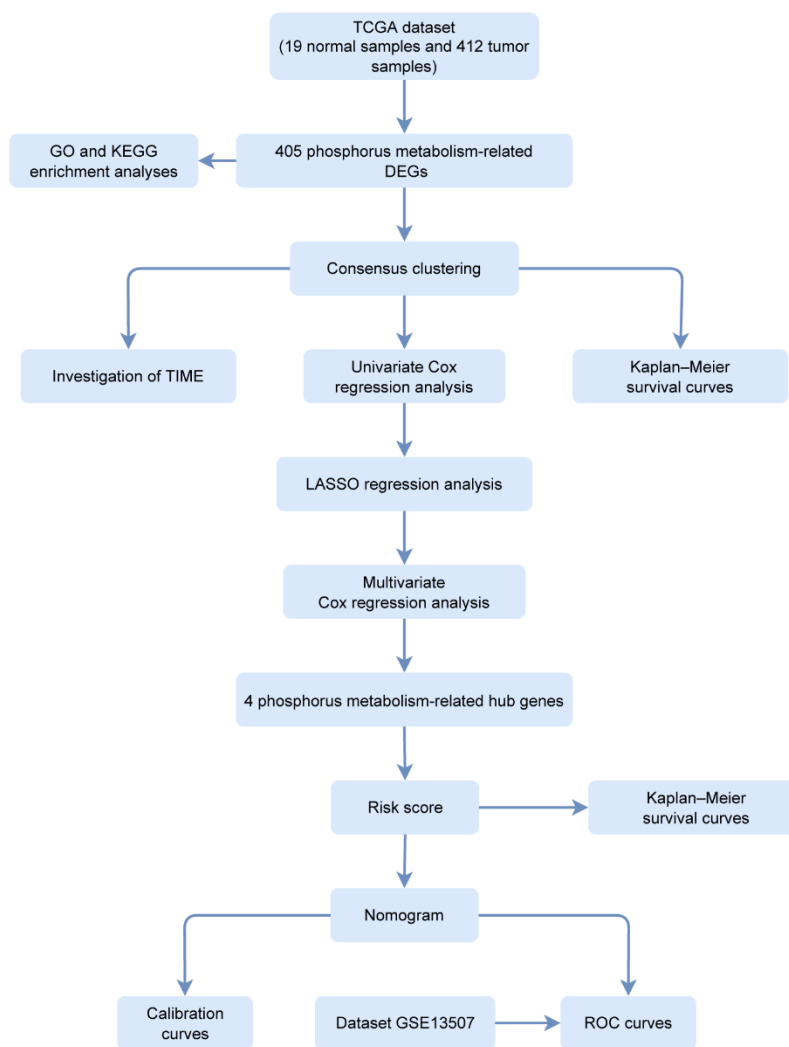
Fig. 1 depicts the workflow of the entire study.

Fig. 1: Flowchart of the entire study process.

Data Collection and Processing

We downloaded clinical information and gene transcriptome data containing 19 normal samples and 412 tumor samples from The TCGA (Cancer Genome Atlas) database (https://portal.gdc.cancer.gov/) for gene differential analysis of phosphorus metabolism-related genes and the development of a reliable prognostic model. Phosphorus metabolism-related genes were derived from the Molecular Signatures Database (MSigDB, https://www.gsea-msigdb.org/gsea/msigdb/). We utilized the "DESeq2" package to uncover differentially expressed genes (DEGs) between normal samples and tumor samples, with the threshold for differentially expressed genes set at adjusted *P*-value < 0.05 and |log2-fold change| > 1. The intersection between DEGs and phosphorus metabolism-related genes is considered as phosphorus metabolism-related DEGs. The GSE13507 microarray dataset (9), containing clinical information for 165 bladder cancer samples, was acquired from the Gene Expression Omnibus (GEO) database (https://www.ncbi.

nlm.nih.gov/geo/). In both datasets, duplicate samples and data with missing values were removed.

Enrichment Annotation Analysis

Phosphorus metabolism-related DEGs obtained from the analysis of the previous step were then analyzed by GO (Gene Ontology) and KEGG (Kyoto Encyclopedia of Genes and Genomes) enrichment analyses; these were performed using the Metascape database (10), and results with $P <$ 0.05 were considered significant. The interactions of phosphorus metabolism-related genes were also visualized with this tool.

Cluster Analysis

We employed the "ConsensusClusterPlus" package for consensus clustering based on phosphorus metabolism-related genes, and Kaplan-Meier survival analysis was applied to compare the OS (overall survival) of different clusters. The expression levels and clustering of phosphorus metabolism-related genes and other clinical features are presented using a heatmap.

Estimation of the Proportions of Immune Cell Infiltrations

To explore the relationship between phosphorus metabolism-related clusters and the TIME, we performed the TIME analysis method on samples from the TCGA dataset. This analysis was conducted using the "CIBERSORT" algorithm (11). The proportions of 22 immune infiltrating cells in cluster 1 and cluster 2 were compared.

Detection of Prognosis-Associated Genes

To remove redundant factors and prevent overfitting, we performed LASSO (least absolute shrinkage and selection operator) regression using the "glmnet" package in the R environment. Univariate Cox regression analysis and multivariate Cox regression analysis were used to screen prognosis-associated genes; exclusion criteria were set as HR (Hazard ratio) = 1 or $P > 0.05$. The difference in OS between prognosis-associated phosphorus metabolism genes at high and low levels of expression was also determined using Kaplan-Meier survival analysis.

Calculation of the Risk Score

The risk score for each sample was generated depending on the expression levels of prognosis-associated genes involved in phosphorus metabolism and coefficients. We calculated risk scores using the formula below (12).

$$\text{Risk Score} = \sum_{i=1}^{n} \text{Coefficient}_i \times \text{Expression}_i$$

Samples from TCGA dataset were separated into different groups based on the risk scores. We performed Kaplan-Meier survival analysis on these two different groups, and the OS of groups with different risk scores were compared.

Development and Validation of a Nomogram

We randomly split the TCGA dataset into a training set and a test set. The prognostic model was built using the training set, incorporating risk scores and clinical characteristics. Subsequently, a nomogram was generated. The nomogram was validated using ROC (receiver operating characteristic) curves based on the TCGA test set. In addition, we also validated the model using the dataset GSE13507. We performed these analyses using the "rms" package and "survivalROC" package in R.

Statistical analysis

R software (version 4.2.1) and R packages were employed for statistical analysis. Prognosis-associated genes were screened using LASSO regression analysis, univariate and multivariate Cox regression analysis; multivariate Cox regression analysis was also applied in the construction of the prognostic model. Kaplan-Meier log-rank test was applied to compare OS between different groups. Wilcoxon rank-sum test was utilized to evaluate independent nonparametric samples.

Results

Phosphorus Metabolism-Related DEGs between Normal and Tumor Samples

We obtained 1,427 phosphorus metabolism-related genes from the MSigDB, and we per-

formed differential gene expression analysis on these genes based on their expression levels in the TCGA dataset. Finally, we identified 405 phosphorus metabolism-related DEGs using in-clusion thresholds (|log2 fold change| > 1 and adjusted $P < 0.05$), including 205 upregulated and 200 down-regulated genes (Fig. 2A, Supplementary Table 1).

Table 1: Univariate Cox regression analysis of phosphorus metabolism-related DEGs

Hub Genes	HR (95% CI for HR)	P-value
HDAC4	1.3 (1.1-1.6)	0.01
LIME1	0.71 (0.58-0.86)	0.00077
CDK5RAP3	0.83 (0.71-0.96)	0.015
PPP1R16A	0.94(0.9-0.99)	0.019
PPP1R35	0.95(0.92-0.99)	0.0064
LRP8	1.2(1.1-1.3)	0.0043
HEXIM2	0.66(0.48-0.91)	0.011
IL31RA	1.6(1.1-2.2)	0.0057
SPDYA	0.047(0.008-0.28)	0.00078
NTF3	0.54(0.32-0.91)	0.021
PPARGC1B	0.74(0.57-0.95)	0.019
SRCIN1	0.91(0.85-0.98)	0.018
CLN3	0.18(0.038-0.82)	0.027
CHRM5	8.9(1.9-42)	0.0055
MST1R	0.96(0.94-0.98)	0.00042
EPO	1.2(1.1-1.5)	0.0099
IFNB1	0.096(0.011-0.85)	0.035
ADRA2B	1.2(1.1-1.3)	0.0032
BMPER	1.3(1.1-1.5)	0.011

Functional Enrichment Analysis of Phosphorus Metabolism-Related DEGs

GO and KEGG analyses were then applied to phosphorus metabolism-related DEGs. The identified genes were significantly associated with various biological processes, including positive regulation of phosphate metabolic process, regulation of kinase activity, regulation of MAPK cascade, negative regulation of phosphate metabolic process, cell population proliferation, positive regulation of cell migration, phosphorylation, regulation of cell activation, tube morphogenesis, etc. (Fig. 2B, $P < 0.05$). In the realm of molecular function, the enriched GO terms primarily centered around kinase regulator activity, kinase binding, and protein kinase binding (Fig. 2C, $P < 0.05$). Within the cellular component category, phosphorus metabolism-related DEGs exhibited significant enrichment in the receptor complex, protein kinase complex, and cell body (Fig. 2D, $P < 0.05$). KEGG pathway analysis revealed significant enrichment in cytokine-cytokine receptor interaction, cell cycle, focal adhesion, EGFR tyrosine kinase inhibitor resistance, transcriptional misregulation in cancer, TGF-beta signaling pathway, hematopoietic cell lineage, cGMP-PKG signaling pathway, osteoclast differentiation, colorectal cancer, cAMP signaling pathway, etc. (Fig. 2E, $P < 0.05$).

Explorations of Phosphorus Metabolism-Associated Clusters

Utilizing the expression profiles of genes associated with phosphorus metabolism, we conducted consensus clustering analysis through the "ConsensusClusterPlus" package, classifying patients in the TCGA dataset into two distinct groups (Fig. 2F). The heatmap visualized the expression levels of phosphorus metabolism-related genes and other clinical features, revealing marked distinctions between the two clusters (Fig. 3A). The OS of patients in cluster 1 was notably superior to that of cluster 2, as revealed by Kaplan-Meier survival analysis (Fig. 3B).
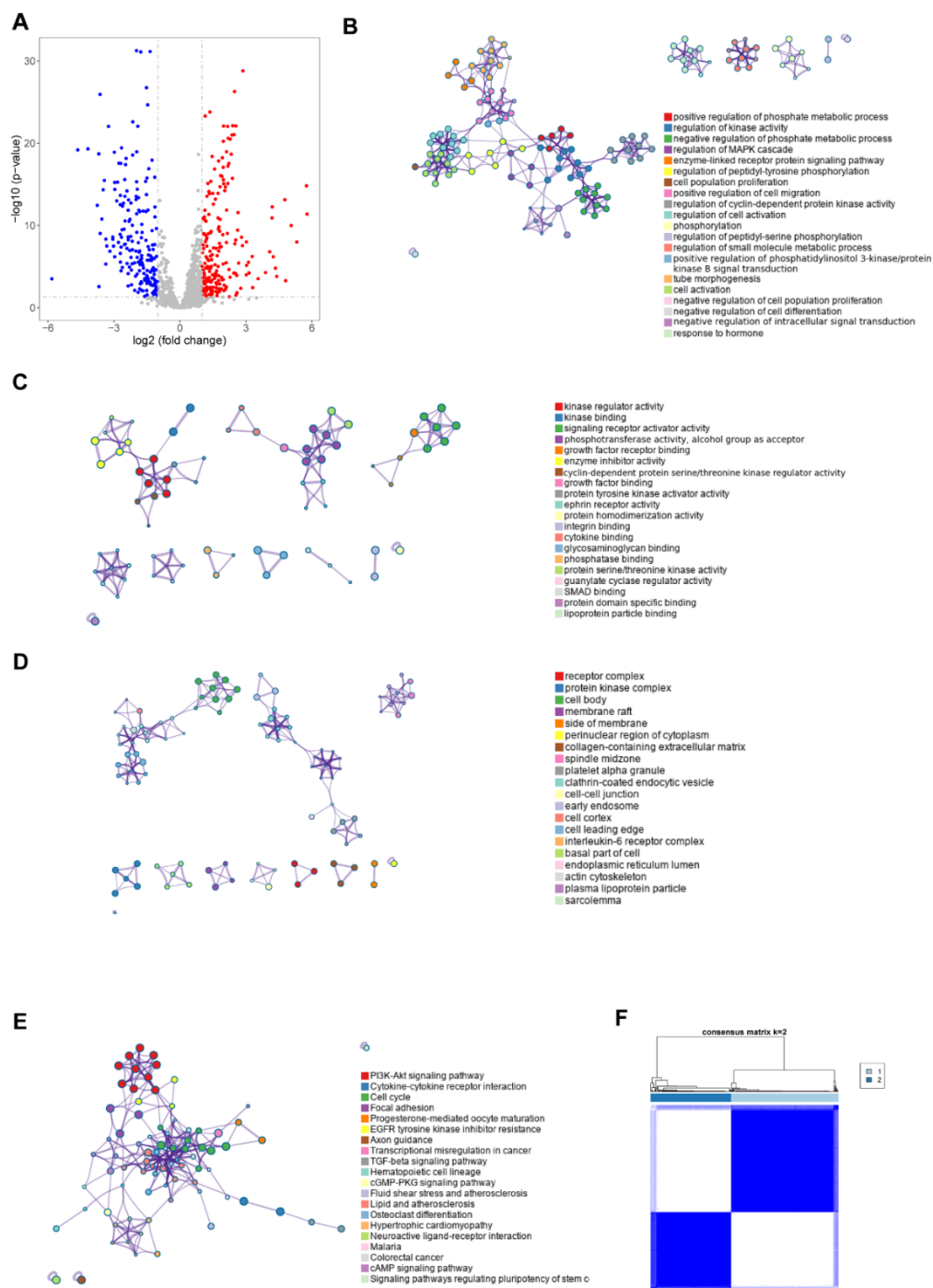
Fig. 2: Investigation of DEGs related to phosphorus metabolism. **(A)** Differentially expressed genes between normal and tumor samples displayed as a volcano map. Results of GO **(B-D)** and KEGG **(E)** enrichment analyses are exhibited using enrichment networks, and the same-colored dots represent genes of the same pathway. The results of GO enrichment analysis are presented categorically, representing (**B**) biological processes (BP), (**C**) molecular functions (MF) and (**D**)cellular components (CC). **(F)** Bladder cancer patients were divided into two groups utilizing consensus clustering.
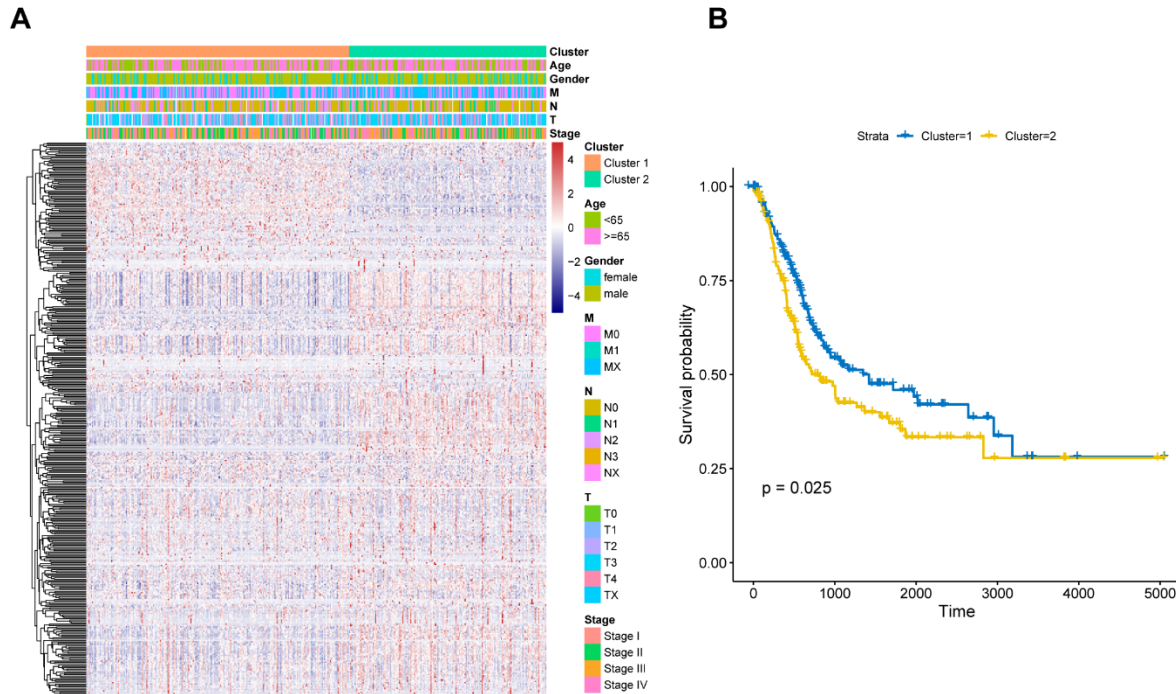
Fig. 3: Characteristics of the two clusters. **(A)** The heatmap displays the clinical characteristics of the two clusters based on phosphorus metabolism-related DEGs. **(B)** Kaplan–Meier survival curves of the patients in different clusters.

Association of Phosphorus Metabolism-Related Clusters with Immune Cell Infiltration

To further investigate the relationship between phosphorus metabolism-associated clusters and the TIME, we compared the proportions of infiltration of 22 types of immune cells (Fig. 4A, Fig. 4B). The infiltrating levels of naive B cells, resting mast cells, monocytes, plasma cells, naive CD4+ T cells, gamma delta T cells, and regulatory T cells (Tregs) were significantly higher in cluster 1. Cluster 2 showed predominant infiltration by macrophages M0, macrophages M1, macrophages M2, and neutrophils.

Identification of Prognosis-Related Hub Genes and Calculation of a Risk Score

We conducted univariate Cox regression analysis based on 405 phosphorus metabolism-related DEGs in TCGA dataset, and 19 genes that met the criteria of HR $\neq$ 1 and $P < 0.05$ were selected for the next step of the analysis (Table 1). LASSO regression analysis was utilized to remove redundant genes and minimize overfitting (Fig. 5A, Fig. 5B). Following LASSO regression analysis, four genes were identified as hub phosphorus metabolism-related genes (Table 2).

Table 2: Expression values of 4 hub phosphorus metabolism-related DEGs

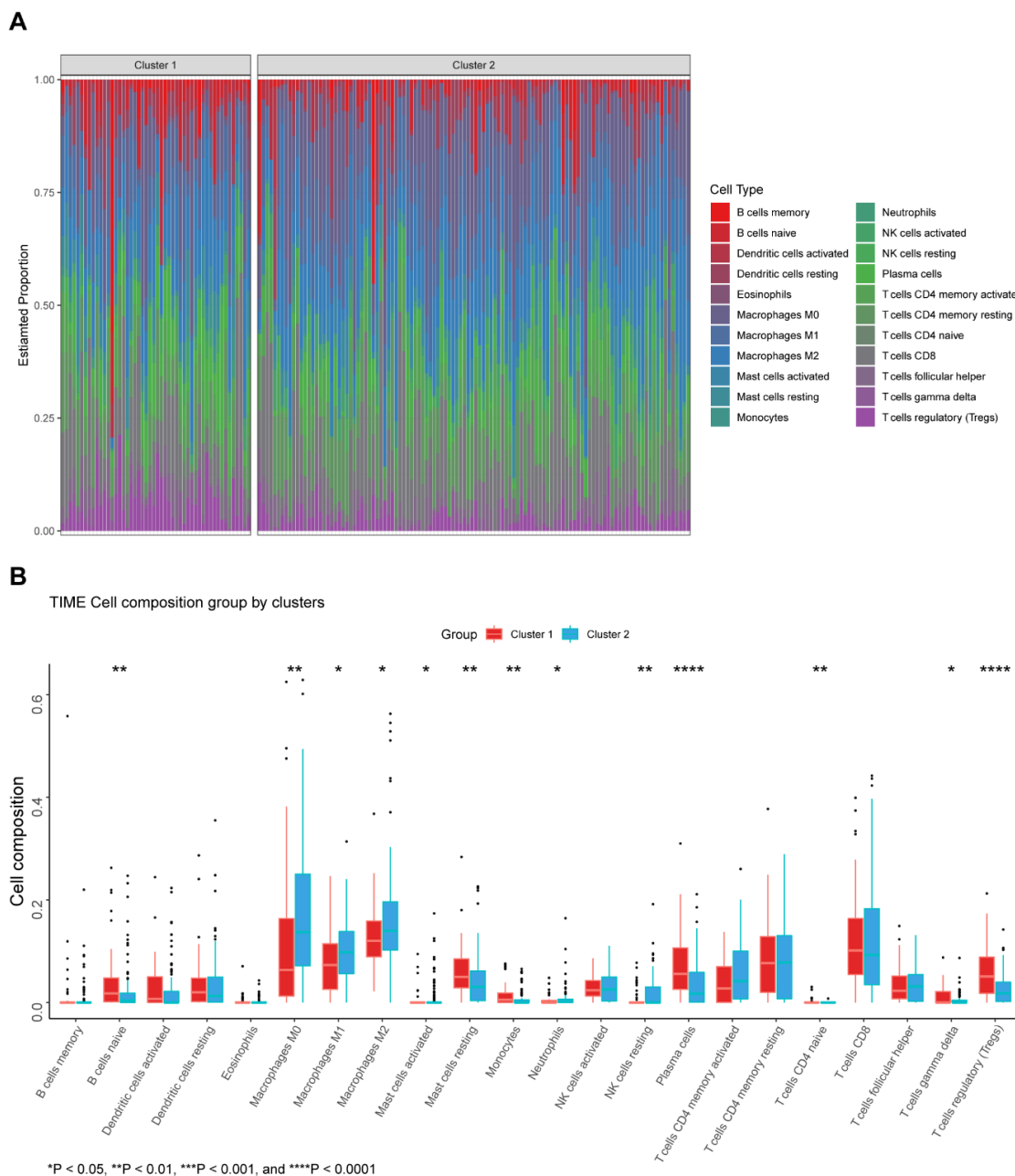| *Genes*	*log2FoldChange*	*P.adj*	*Change*
LIME1	2.035280216	5.92E-15	upregulate
LRP8	1.947363767	1.35E-09	upregulate
SPDYA	1.439611929	1.48E-06	upregulate
MST1R	1.240745607	0.003677095	upregulate

Fig. 4: Exploration of tumor immune microenvironment. **(A)** The abundance of tumor-infiltrating immune cells. **(B)** The proportion of tumor-infiltrating immune cells in cluster 1 and cluster 2 were compared.

The distinctions in OS between the high- and low- expression groups of metabolism-related hub genes were demonstrated by Kaplan-Meier survival curves (Fig. 5C-F). When setting the median of *LRP8* expression as the demarcation for high and low expression, there was no statistical difference in OS between the two groups. However, after determining the optimal cut-off value for classifying the high- and low- expression groups, a significant distinction was confirmed. (Fig. 5G, Fig. 5H).
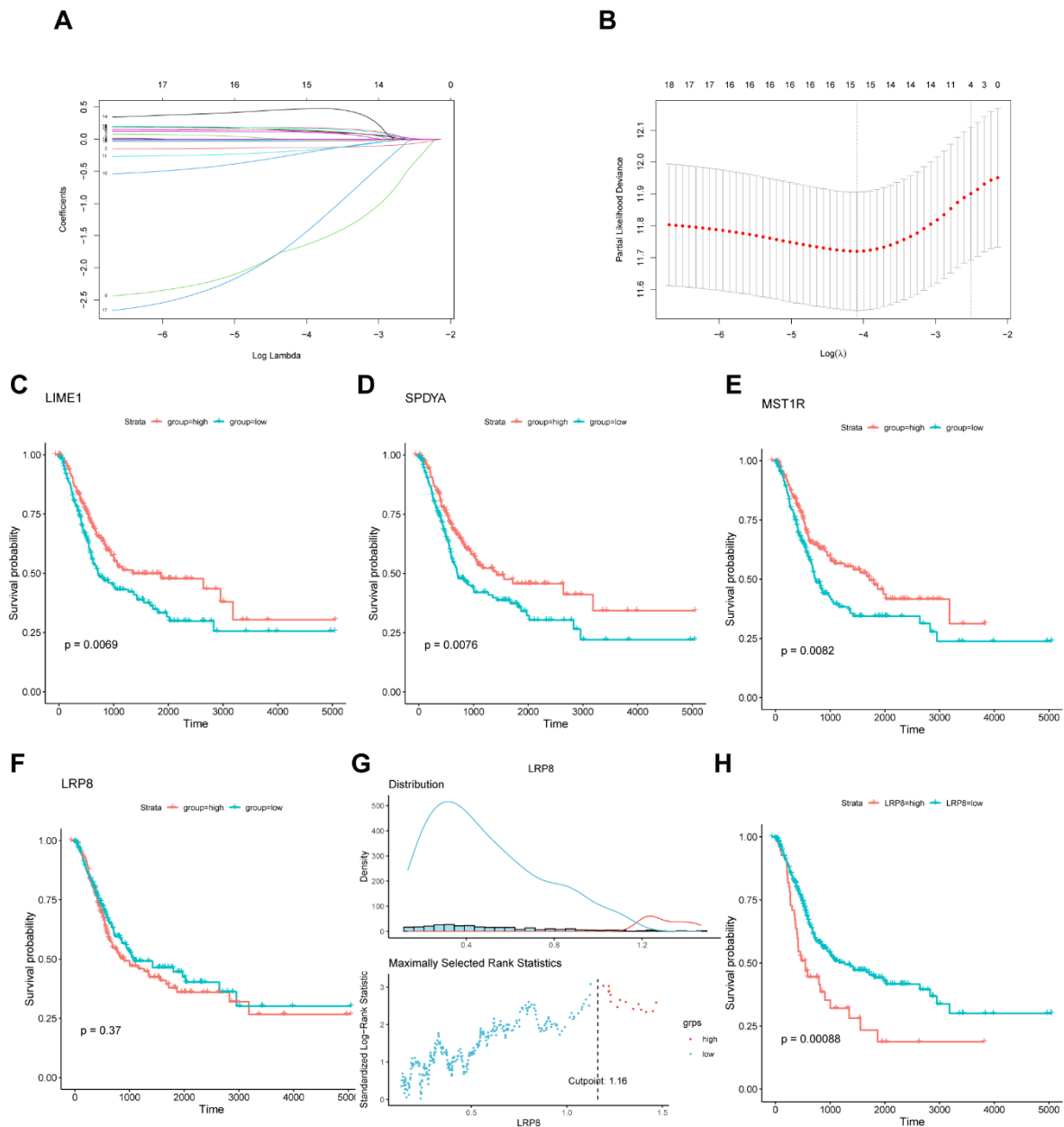
Fig. 5: Prognostic value of phosphorus metabolism-related genes. **(A, B)** Redundant factors were removed using LASSO regression. **(C-F)** Kaplan-Meier survival curves of patients with different expression levels of phosphorus metabolism-related hub genes, grouped according to the median gene expression value. **(G)** The optimal cut-off point to divide the high- and low- expression groups was chosen. **(H)** Kaplan-Meier survival curves of patients with different expression levels of LRP8, grouped according to the optimal cut-off point.

Within cluster 1, the expression levels of *LIME1(Lck Interacting Transmembrane Adaptor 1)* and *SPDYA (Speedy/RINGO Cell Cycle Regulator Family Member A)* were upregulated, while in cluster 2, *LRP8 (Low-density Lipoprotein Receptor-related Protein 8)* exhibited increased expression. However, there was no significant difference in the expression level of *MST1R (Macrophage Stimulating 1 Receptor)* between the two groups (Fig. 6A-D).
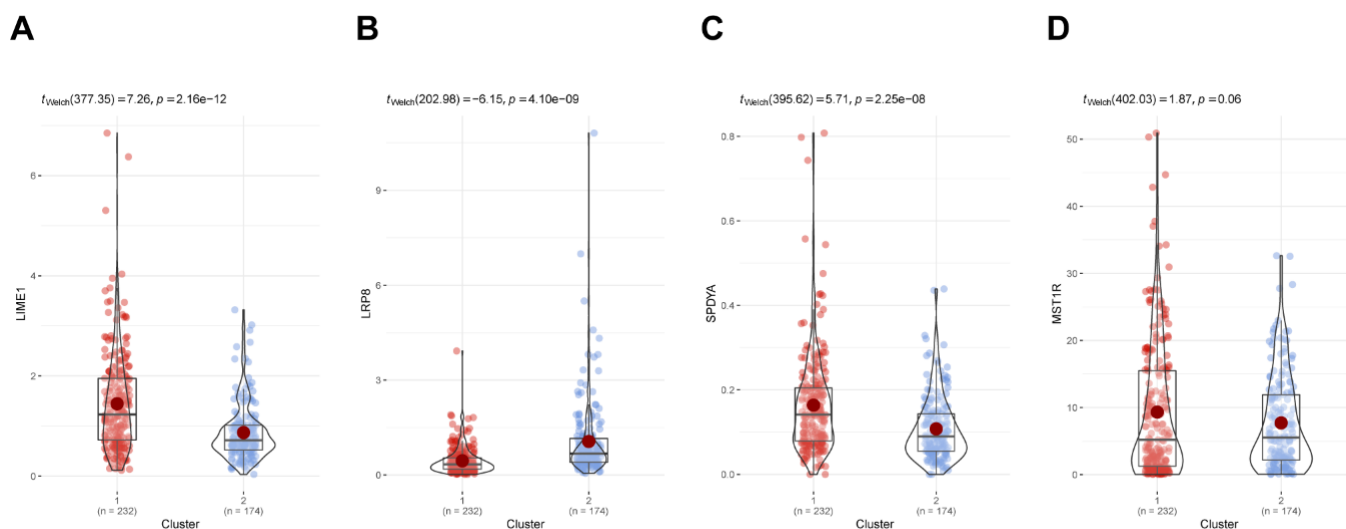
Fig. 6: (A-D) The expression levels of phosphorus metabolism-related hub genes in different clusters.

Multivariate Cox regression was then applied (Fig. 7A), followed by the calculation of risk scores using the formula: Risk Score = (-0.25289 × *LIME1*) + (0.13663×*LRP8*) + (-2.11592 × *SPDYA*) + (-0.04274 × *MST1R*). Subsequent survival analysis revealed significantly better OS in the low-risk group compared to the high-risk group, with the division based on the median of risk scores (Fig. 7B). The phosphorus metabolism-related risk score was considered an independent prognostic factor (Fig. 7C).

Establishment and Validation of a Nomogram Based on Phosphorus Metabolism-Related Risk Score
For the prediction of prognosis in BLCA patients, we conducted the construction of a nomogram based on the TCGA training dataset (Fig.

7D). The risk score involved in phosphorus metabolism-related genes, age, gender, T stage, and N stage were included in the nomogram as predictors. Notably, the risk score held the most substantial weight in prognostic prediction. The C-index for the nomogram based on the training cohort reached 0.70923316. We then validated the performance of the nomogram using calibration and ROC curves. Calibration curves determined the reliability of the nomogram on 1 - and 5-year OS predictions (Fig. 7E, Fig. 7F). Time-dependent ROC curves based on TCGA testing cohort and the GEO cohort were developed; the AUC (area under the curve) values for the 1-year and 5-year OS were 0.825 and 0.714, respectively (Fig. 7G), based on TCGA testing cohort; and 0.91 and 0.846, respectively, based on the GEO cohort (Fig. 7H).
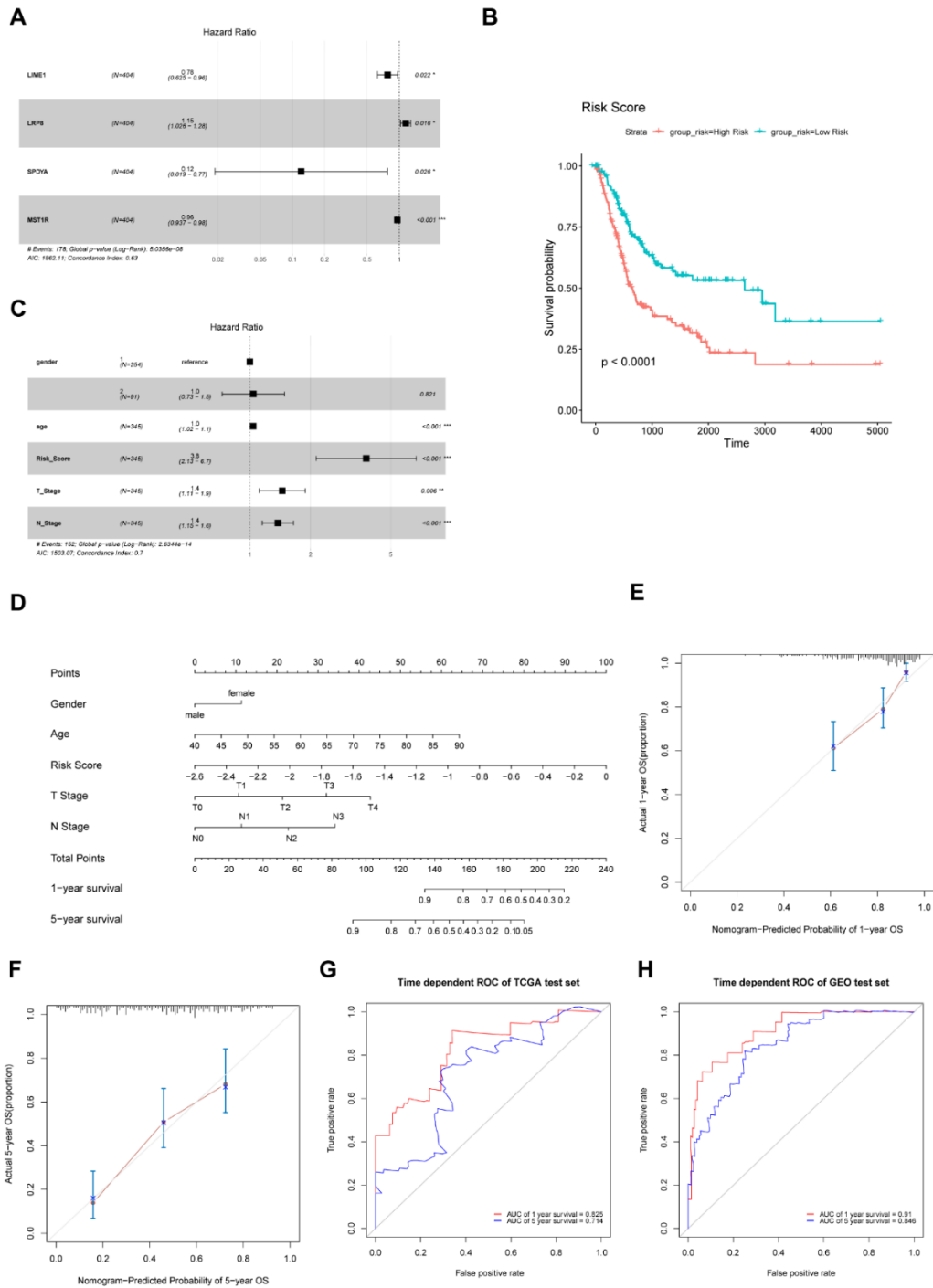
Fig. 7: Establishment and validation of prognostic model. **(A)** A Forest map of phosphorus metabolism-related hub genes, and univariate Cox regression analysis was used to calculate hazard ratios (HRs) and *P*-values. **(B)** The OS of the low-risk group was significantly longer than that of the high-risk group, as determined by Kaplan-Meier survival analysis. **(C)** A Forest map of risk score and other clinical features. **(D)** Nomogram based on phosphorus metabolism-related risk score. **(E, F)** Calibration curve of the nomogram based on TCGA training cohort. **(G, H)** The time-dependent ROC curves of TCGA testing cohort and the GEO cohort.

Discussion

In the present study, 405 phosphorus metabolism-related DEGs were identified. Subsequently, a consensus clustering analysis based on these DEGs was performed, and the OS of different clusters was compared. Furthermore, we investigated variations in the tumor immune microenvironment among patients in different clusters. Multiple statistical methods were sequentially applied to these phosphorus metabolism-related DEGs, leading to the identification of four genes (*LIME1, LRP8, SPDYA,* and *MST1R*) involved in the prognosis of BLCA patients. Risk scores were computed based on the expression levels of these genes, enabling the establishment of a prognostic model. The model was visualized as a nomogram, incorporating risk scores and other prognosis-associated features. We demonstrated the acceptable performance of this nomogram with calibration curves and ROC curves. Notably, we have, for the first time, confirmed the association between phosphorus metabolism-related genes and the prognosis of bladder cancer patients. We identified potential therapeutic targets and explored differences in the immune microenvironment among distinct clusters of phosphorus metabolism-related genes. Additionally, we constructed a prognostic model related to phosphorus metabolism, aiming to assist in predicting the prognosis of bladder cancer patients and guiding the selection of treatment strategies.

BLCA accounts for approximately 573,000 new cases and 21,300 deaths annually, making it one of the most prevalent malignancies posing a significant threat to human health (1). The intricate biological mechanisms underlying the initiation, development, and metastasis of bladder cancer remain incompletely understood, and current treatment options are constrained. Phosphorus, associated with vital pathways, plays a multifaceted role beyond energy generation, storage, and blood buffering. Phosphorus metabolism is implicated in the regulation of gene transcription, activation of enzyme catalysis, signaling pathways

in signal transduction, and immune responses (13). It has been previously documented that serum levels of phosphorus are elevated in cancer patients compared to normal individuals (14). There are also hypotheses suggesting that tumor cells tend to metastasize to phosphorus-rich microenvironments (6). High phosphorus intake increases cancer risk by activating the PI3K signaling pathway, as excess phosphate in cells leads to abnormal activation of the IP3/Akt signaling pathway, explaining its association with various types of cancer (3). It seems that abnormal phosphorus metabolism is associated with the biological processes of tumor cells.

Bladder cancer, characterized by a high mutational load, exhibits increased sensitivity to immunotherapy. The immune checkpoint pathway serves as an intrinsic mechanism for regulating autoimmunity in the context of physiological immune responses, and tumor cells can exploit this pathway to facilitate immune evasion (15). This study conducted a comparative analysis of the TIME within two distinct phosphorus metabolism-related clusters, aiming to identify potential therapeutic strategies and additional prognostic factors. Our findings revealed that the cluster with a better prognosis demonstrated heightened infiltration of naive B cells and plasma cells. Tumor-infiltrating B cells and plasma cells appeared to play a positive role in the prognosis of the majority of cancer patients (16). The anti-tumor effect attributed to B cells may stem from their capability to produce IgG or IgA antibodies targeting tumor antigens (17). According to previous findings, CD4+ Th1 cells and gamma delta-T cells are generally engaged in type I immune responses, which may lead to a better prognosis for lung cancer patients (18). We speculate that a similar scenario may exist for patients with BLCA. CD4+ T cells play an essential role in anti-tumor immunity by promoting cytotoxic T cell activation and the conversion of B cells into plasma cells or memory B cells (19), so it is not difficult to understand why the proportion of naive CD4+ T clusters1 is higher. Tregs suppress the anti-tumor immune response of effector T cells

and mediate the development of immune tolerance to tumor cells, which often results in a worse prognosis for patients (20). Interestingly, our study reveals inconsistencies with these findings, and further investigation is necessary to determine the exact reasons for these disparities. Monocytes may directly kill tumor cells, and this mechanism occurs through cytokine-mediated cell death and phagocytosis (21). Macrophages directly or indirectly suppress T cell expression with anti-tumor activity in the TIME. Moreover, macrophages can secrete molecules that contribute to the metastasis of tumor cells, which may be one of the reasons why cluster 1 has a better prognosis than cluster 2 (22). A high abundance of mast cells in the tumor immune microenvironment is considered to be an indicator of better prognosis in breast, prostate and lung cancers (23), and our study suggests that it may be similar in BLCA.

Four hub genes (*LIME1, LRP8, SPDYA,* and *MST1R*) were identified as biomarkers of phosphorus metabolism in BLCA. *LIME1* exhibits upregulated expression in tumor tissue samples, consistent with observations in prostate cancer (24). As previously reported, *LIME1* is predominantly expressed in T and B cells, particularly in effector T cells, and its product is a raft-associated transmembrane protein (25). The notable association of *LIME1* with the regulation of T cell activation underscores its significance in immune response mechanisms. (26). *LIME1* acts as a docking protein to recruit signaling molecules, which occurs after the phosphorylation of tyrosine residues in its cytoplasmic tail upon TCR stimulation (27). *LIME1* is also involved in inflammatory pathways, such as MAPK signaling (28), which is concordant with the results of functional enrichment analysis in this study. Besides, *LIME1* also plays a role in Lck activation and CD55-mediated signals; therefore, it may also be involved in cisplatin resistance. The association of *LIME1* with genes engaged in DNA repairs, such as *MLH1 (MutL Protein Homolog 1)* and *BRCA1 (Breast Cancer 1)* (29), may be one of the reasons why *LIME1* is linked to a better prognosis for bladder cancer patients. Within the scope of our research, we observed an upregulation of *LPR8* expression in bladder cancer tumor tissues. Previous investigations in the realm of breast cancer similarly reveal an increased expression pattern, associating its upregulation with an unfavorable prognosis for individuals with breast cancer (30). *LRP8* is a member of the low-density lipoprotein receptor-related protein (LRP) family that possesses conserved structural domains, such as low-density lipoprotein repeat sequences and EGF receptor-like structural domains (31). Its involvement in Wnt signaling is notable, where *LRP8* can either inhibit or activate Wnt signaling through different regulatory mechanisms. Amplification and overexpression of *LRP8* have been linked to lung cancer, and its role in carcinogenesis may stem from these regulatory interactions (32). *MiR-1262* is an upstream regulatory factor of *LRP8*, which can control cell proliferation, invasion, and migration (30). According to the previous description, *LRP8* is an oncogene in triple-negative breast cancer, and its upregulated expression can make the malignant cells turn to be poorly differentiated, resulting in chemotherapy insensitivity (33). The Speedy/Ringo family, which includes SPDYA (also known as Spy1), plays a crucial role in regulating cell proliferation and survival by atypically activating cell cycle protein-dependent kinases (34). *SPDYA* exhibits elevated expression in epithelial ovarian cancer and colorectal tissues, and we have observed a similar trend in bladder cancer (35). In colorectal cancer, high levels of Spy1 protein would typically result in shorter survival for patients (36), contrary to our findings, which may be due to a different mechanism in bladder cancer than in colorectal cancer and therefore requires further study. *MST1R*, as a tumor suppressor gene, is upregulated in the tumor tissues of various malignant cancers such as bladder cancer, breast cancer, and lung adenocarcinoma (37, 38). The product of *MST1R* is a molecule located on the cell surface for binding macrophage-stimulating proteins. *MST1R* is activated by autophosphorylation of its kinase catalytic domain upon binding to macrophage-stimulating protein, thereby driving tumor progression, adhesion,

proliferation, and apoptosis (39, 40). Downregulated expression levels of *MST1R* are associated with pancreatic tumor shrinkage, altered macrophage polarization, and increased proportions of T cell infiltration. (40). High expression levels of *MST1R* usually lead to worse prognosis in pancreatic, lung and gastric cancers (41-43). The association of *SPDYA* and *MST1R* with prognosis in other cancers is inconsistent with our findings, and we speculate that it may be due to the unique pathological type of BLCA.

However, this study has some limitations. Due to the limited sample size, we did not analyze additional data to obtain more comprehensive results. As this study is based on bioinformatics, further laboratory validation is necessary. Additionally, further research is needed to confirm the mechanisms of action of phosphorus metabolism-related genes in bladder cancer.

Conclusion

We successfully identified phosphorus metabolism-related hub genes associated with prognosis and compared differences in TIME between clusters. These phosphorus metabolism-related hub genes could serve as novel biomarkers for predicting bladder cancer prognosis and as potential therapeutic targets. Subsequently, we used these hub genes to calculate risk scores and constructed a prognostic model in combination with other important clinical features; the model showed acceptable levels of performance. The nomogram based on phosphorus metabolism-related risk score may provide a new rationale for the choice of treatment options for different patients.

Journalism Ethics considerations

Ethical issues (Including plagiarism, informed consent, misconduct, data fabrication and/or falsification, double publication and/or submission, redundancy, etc.) have been completely observed by the authors.

Availability of data and materials

Datasets analyzed in this study are open to the public and can be found in TCGA (https://portal.gdc.cancer.gov/) and the GEO (https://www.ncbi. nlm.nih.gov/geo/) databases.

Acknowledgements

Conflict of Interests

The authors declare that they have no competing interests.

References

1. Sung H, Ferlay J, Siegel RL, et al (2021). Global cancer statistics 2020: GLOBOCAN estimates of incidence and mortality worldwide for 36 cancers in 185 countries. *CA Cancer J Clin*, 71(3):209-249.

2. Miranda AF, Howard JM, McLaughlin M, et al (2021). Metastasis-directed radiation therapy after radical cystectomy for bladder cancer. *Urol Oncol,* 39 (11):790 e1-790.e7.

3. Venturelli S, Leischner C, Helling T, et al (2022). Minerals and Cancer: Overview of the Possible Diagnostic Value. *Cancers (Basel),* 14(5):1256.

4. Lacerda-Abreu MA, Dick CF, Meyer-Fernandes JR (2022). The Role of Inorganic Phosphate Transporters in Highly Proliferative Cells: From Protozoan Parasites to Cancer Cells. *Membranes (Basel),* 13 (1):42.

5. Brown RB, Bigelow P, Dubin JA (2023). Breast Cancer and Bone Mineral Density in a U.S. Cohort of Middle-Aged Women:

Associations with Phosphate Toxicity. *Cancers (Basel),* 15 (20): 5093.

6. de Carvalho CC, Caramujo MJ (2012). Tumour metastasis as an adaptation of tumour cells to fulfil their phosphorus requirements. *Med Hypotheses,* 78 (5):664-7.

7. Castillo SP, Rebolledo RA, Arim M, et al (2023). Metastatic cells exploit their stoichiometric niche in the network of cancer ecosystems. *Sci Adv,* 9 (50): eadi7902.

8. Lacerda-Abreu MA, Russo-Abrahão T, Rocco-Machado N, et al (2021). Hydrogen Peroxide Generation as an Underlying Response to High Extracellular Inorganic Phosphate (Pi) in Breast Cancer Cells. *Int J Mol Sci,* 22(18):10096.

9. Lee JS, Leem SH, Lee SY, et al (2010). Expression signature of E2F1 and its associated genes predict superficial to invasive progression of bladder tumors. *J Clin Oncol,* 28 (16):2660-7.

10. Zhou Y, Zhou B, Pache L, et al (2019). Metascape provides a biologist-oriented resource for the analysis of systems-level datasets. *Nat Commun,* 10 (1):1523.

11. Newman AM, Liu CL, Green MR, et al (2015). Robust enumeration of cell subsets from tissue expression profiles. *Nat Methods,* 12 (5):453-7.

12. Sullivan LM, Massaro JM, D'Agostino RB, Sr. (2004). Presentation of multivariate data for clinical use: The Framingham Study risk score functions. *Stat Med,* 23 (10):1631-60.

13. Calvo MS, Lamberg-Allardt CJ (2015). Phosphorus. *Adv Nutr,* 6 (6):860-2.

14. Papaloucas CD, Papaloucas MD, Kouloulias V, et al (2014). Measurement of blood phosphorus: a quick and inexpensive method for detection of the existence of cancer in the body. Too good to be true, or forgotten knowledge of the past? *Med Hypotheses,* 82 (1):24-5.

15. Donin NM, Lenis AT, Holden S, et al (2017). Immunotherapy for the Treatment of Urothelial Carcinoma. *J Urol,* 197 (1):14-22.

16. Wouters MCA, Nelson BH (2018). Prognostic Significance of Tumor-Infiltrating B Cells and Plasma Cells in Human Cancer. *Clin Cancer Res,* 24 (24):6125-6135.

17. Fridman WH, Petitprez F, Meylan M, et al (2021). B cells and cancer: To B or not to B? *J Exp Med,* 218(1):e20200851.

18. Wang SS, Liu W, Ly D, et al (2019). Tumor-infiltrating B cells: their role and application in anti-tumor immunity in lung cancer. *Cell Mol Immunol,* 16 (1):6-18.

19. Okita Y, Ohira M, Tanaka H, et al (2015). Alteration of CD4 T cell subsets in metastatic lymph nodes of human gastric cancer. *Oncol Rep,* 34 (2):639-47.

20. Ebert LM, Tan BS, Browning J, et al (2008). The regulatory T cell-associated transcription factor FoxP3 is expressed by tumor cells. *Cancer Res,* 68 (8):3001-9.

21. Olingy CE, Dinh HQ, Hedrick CC (2019). Monocyte heterogeneity and functions in cancer. *J Leukoc Biol,* 106 (2):309-322.

22. Ruffell B, Coussens LM (2015). Macrophages and therapeutic resistance in cancer. *Cancer Cell,* 27 (4):462-72.

23. Aponte-López A, Muñoz-Cruz S (2020). Mast Cells in the Tumor Microenvironment. *Adv Exp Med Biol,* 1273:159-173.

24. Zheng X, Xu H, Yi X, et al (2021). Tumor-antigens and immune landscapes identification for prostate adenocarcinoma mRNA vaccine. *Mol Cancer,* 20 (1):160.

25. Park I, Son M, Ahn E, et al (2020). The Transmembrane Adaptor Protein LIME Is Essential for Chemokine-Mediated Migration of Effector T Cells to Inflammatiory Sites. *Mol Cells,* 43 (11):921-934.

26. Brdickova N, Brdicka T, Angelisova P, et al (2003). LIME: a new membrane Raft-associated adaptor protein involved in CD4 and CD8 coreceptor signaling. *J Exp Med,* 198 (10):1453-62.

27. Hur EM, Son M, Lee OH, et al (2003). LIME, a novel transmembrane adaptor protein, associates with p56lck and mediates T cell activation. *J Exp Med,* 198 (10):1463-73.

28. Li SC, Kuo HC, Huang LH, et al (2021). DNA Methylation in LIME1 and SPTBN2 Genes Is Associated with Attention Deficit in Children. *Children (Basel),* 8 (2):92.

29. Bommhardt U, Schraven B, Simeoni L (2019). Beyond TCR Signaling: Emerging Functions of Lck in Cancer and Immunotherapy. *Int J Mol Sci,* 20 (14): 3500.

30. Li L, Qu W-H, Ma H-P, et al (2022). LRP8, modulated by miR-1262, promotes tumour progression and forecasts the prognosis of patients in breast cancer. *Arch Physiol Biochem,* 128 (3):657-665.

31. Rey JP, Ellies DL (2010). Wnt modulators in the biotech pipeline. *Dev Dyn,* 239 (1):102-14.

32. Garnis C, Campbell J, Davies JJ, et al (2005). Involvement of multiple developmental genes on chromosome 1p in lung tumorigenesis. *Hum Mol Genet,* 14 (4):475-82.

33. Lin CC, Lo MC, Moody R, et al (2018). Targeting LRP8 inhibits breast cancer stem cells in triple-negative breast cancer. *Cancer Lett,* 438:165-173.

34. McAndrew CW, Gastwirt RF, Donoghue DJ (2009). The atypical CDK activator Spy1 regulates the intrinsic DNA damage response and is dependent upon p53 to inhibit apoptosis. *Cell Cycle,* 8 (1):66-75.

35. Lu S, Liu R, Su M, Wei Y, et al (2016). Spy1 participates in the proliferation and apoptosis of epithelial ovarian cancer. *J Mol Histol,* 47 (1):47-57.

36. Jin Q, Liu G, Bao L, et al (2018). High Spy1 expression predicts poor prognosis in colorectal cancer. *Cancer Manag Res,* 10:2757-2765.

37. An W, Kang JS, Oh S, et al (2023). MST1R as a potential new target antigen of chimeric antigen receptor T cells to treat solid tumors. *Korean J Physiol Pharmacol,* 27 (3):241-256.

38. Khan M, Hearn K, Parry C, et al (2023). Mechanism of Antitumor Effects of Saffron in Human Prostate Cancer Cells. *Nutrients,* 16 (1):114.

39. Jeong BC, Oh SH, Lee MN, et al (2020). Macrophage-Stimulating Protein Enhances Osteoblastic Differentiation via the Recepteur d'Origine Nantais Receptor and Extracellular Signal-Regulated Kinase Signaling Pathway. *J Bone Metab,* 27 (4):267-279.

40. Zou Y, Yuan G, Tan X, et al (2022). Immune-related gene risk score predicting the effect of immunotherapy and prognosis in bladder cancer patients. *Front Genet,* 13:1011390.

41. Kato A, Ng S, Thangasamy A, et al (2021). A potential signaling axis between RON kinase receptor and hypoxia-inducible factor-1 alpha in pancreatic cancer. *Mol Carcinog,* 60 (11):734-745.

42. Milan M, Benvenuti S, Balderacchi AM, et al (2018). RON tyrosine kinase mutations in brain metastases from lung cancer. *ERJ Open Res,* 4(1):00083-2017.

43. Zhou D, Zhu X, Wu X, et al (2021). The effect of splicing MST1R in gastric cancer was enhanced by lncRNA FENDRR. *Exp Ther Med,* 22 (2):798.